Responding to Media Inquiries about Earthquake Triggering Interactions

Fang Fan[1], Lingling Ye[*1,2] , Hiroo Kanamori[3] , and Thorne Lay[4]

Abstract

In the aftermath of a significant earthquake, seismologists are frequently asked questions by the media and public regarding possible interactions with recent prior events, including events at great distances away, along with prospects of larger events yet to come, both locally and remotely. For regions with substantial earthquake catalogs that provide information on the regional Gutenberg–Richter magnitude–frequency relationship, Omori temporal aftershock statistical behavior, and aftershock productivity parameters, probabilistic responses can be provided for likelihood of nearby future events of larger magnitude, as well as expected behavior of the overall aftershock sequence. However, such procedures generally involve uncertain extrapolations of parameterized equations to infrequent large events and do not provide answers to inquiries about long-range interactions, either retrospectively for interaction with prior remote large events or prospectively for interaction with future remote large events. Dynamic triggering that may be involved in such long-range interactions occurs, often with significant temporal delay, but is not well understood, making it difficult to respond to related inquiries. One approach to addressing such inquiries is to provide retrospective or prospective occurrence histories for large earthquakes based on global catalogs; while not providing quantitative understanding of any physical interaction, experience-based guidance on the (typically very low) chances of causal interactions can inform public understanding of likelihood of specific scenarios they are commonly very interested in.

Introduction

Earthquakes are complex phenomena, and the hazards they pose generate keen media and public interest in their occurrence following events that receive attention because of their location or societal impact. Although there is sustained interest in generic questions such as "when will the Big One happen?", there is also widespread interest in specific earthquake interaction scenarios involving questions such as "did event A trigger event B?" or "is event A a foreshock of a bigger event B to come?". The latter questions sometimes focus on very nearby faulting interactions, but very often the question is directed at remote, or even global interactions for which there is empirical support (e.g., Velasco *et al.*, 2008; Parsons *et al.*, 2014). The statistical nature of earthquakes observed over many sequences in a given region enables an empirical probabilistic approach to nearby faulting interactions that is now codified in operational earthquake forecasting (OEF) methods (e.g., Jordan and Jones, 2010; Jordan *et al.*, 2011, 2014; Field *et al.*, 2016). This approach draws upon observations of prior seismic sequences parameterized by the Gutenberg–Richter (G-R) magnitude distribution (Gutenberg and Richter, 1944), the Omori law for temporal decay of aftershock sequences (Utsu *et al.*, 1995),

and an exponential aftershock productivity relation that counts all events in a sequence including secondary aftershocks (e.g., Ogata, 1988).

Parametric forecasting methods have become increasingly sophisticated over time, building from the Reasenberg and Jones (1989) approach and the epidemic-type aftershock sequence (ETAS) models of Ogata (1988) to OEF models that can include specific fault distributions and spatial information in the aftershock forecast (e.g., Field *et al.*, 2017). These approaches are appealing in that they seek to incorporate as much information about past earthquake behavior in a region as possible to probabilistically forecast future behavior. In regions such as California, Japan, Italy, and other well-monitored regions with

1. Guangdong Provincial Key Lab of Geodynamics and Geohazards, School of Earth Sciences and Engineering, Sun Yat-sen University, Guangzhou, China, https://orcid.org/0000-0001-9689-4149 (LY); 2. Department of Earth and Space Sciences, Southern University of Science and Technology, Shenzhen, Guangdong, China; 3. Seismological Laboratory, California Institute of Technology, Pasadena, California, U.S.A., https://orcid.org/0000-0001-8219-9428 (HK); 4. Department of Earth and Planetary Sciences, University of California Santa Cruz, Santa Cruz, California, U.S.A., https://orcid.org/0000-0003-2360-4213 (TL)

*Corresponding author: yell@sustech.edu.cn

© Seismological Society of America

robust earthquake catalogs, this is a sensible approach to addressing local sequence evolution and likelihood of events being foreshocks of future larger events.

Of course, the parametric approach has intrinsic limitations. Individual sequences can deviate from prior tuned parametric behavior, and the forecasting of events that have not been sampled in the recorded catalog is subject to large uncertainties, particularly for large events for which observed G-R relations must be extrapolated. The probabilistic framework can convey a false sense of the degree of quantitative understanding underlying statements about possible future large event activity. The same is true for alternate sophisticated approaches based on tectonic strain-rate frameworks that seek causal interpretations of global seismicity distributions (e.g., Bird and Kreemer, 2015; Kagan, 2017; Bayona Viveros *et al.*, 2019). Exploration of nonparametric approaches to mitigate this concern have been explored (e.g., van der Elst and Page, 2018) and are philosophically akin to the procedure discussed in this study. Practical difficulties in communicating the prospects that larger events may follow a given event, as exemplified by the 2016 Kumamoto sequence in Japan, have prompted changes in how information is communicated to the public (e.g., Kamaya *et al.*, 2017; Hashimoto and Yokota, 2019; Fukushima and Nishikawa, 2020). The OEF approach, whereas now being extended to regional fault systems, also intrinsically provides little information regarding long-range interactions (where large events A and B in the questions above are not within a region of OEF statistical calibration). Given the state of knowledge of long-range interactions, one could honestly answer the media inquiries with a vague "anything can happen" response, or perhaps attempt a more nuanced response grounded in cumulative observations. Here, we explore the latter approach, providing convenient summary catalog attributes, but avoiding probabilistic formality which could convey a false confidence in physical understanding.

Catalog Observations

We utilize the National Earthquake Information Center at U.S. Geological Survey (USGS-NEIC) catalog (see Data and Resources) for global activity from 1920 to 2020. The catalog is likely nearly complete at magnitude 6.0 from 1965 to 2020 (e.g., Kagan, 2003; Michael, 2014; Dascher-Cousineau *et al.*, 2020), and with the International Seismological Centre-Global Earthquake Model (ISC-GEM) catalog embedded in it, is likely nearly complete at magnitude 7.0 from 1920 to 2020 (e.g., Michael, 2014). Thus, we extract from the USGS-NEIC catalog from 1 January 1965 to 2 November 2020 events with magnitude ≥ 6.0, and from 1 January 1920 to 31 December 1964 events with magnitude ≥ 7.0. There are 11,535 earthquakes in this selected catalog used in the following analysis. As our focus is on the available catalog history of events, the time-varying completeness level is just an added level of caveat to summary catalog attributes. Time-varying

precision of magnitude estimates, saturation and roundoff of magnitude measures, and spatial inhomogeneity of catalogs are additional caveats that must be kept in mind.

Suppose we have an earthquake with a magnitude 6.0 or larger, then we call this a target earthquake E_T with magnitude M_{ET}. Let N_{total} be the total number of events in the catalog with the magnitude $M = M_{ET}$. As one decimal place for the magnitude is given by the USGS-NEIC catalog, such as 6.0, 6.1, and so on, we use the magnitude interval of 0.1 for further discussion which refers to the magnitude range of $M_{ET} - 0.05 \leq M < M_{ET} + 0.05$. Then, we have two questions:

1. What percentage of all events with $M = M_{ET}$ in the past were followed by earthquakes with equal or larger magnitude in specified time ΔT and spatial range Δr?
2. What percentage of all events with $M = M_{ET}$ in the past were preceded by earthquakes with smaller or equal magnitude but $M \geq 6.0$ (i.e., cutoff magnitude used in this study) in specified time ΔT and spatial range Δr?

We call (1) and (2), prospective and retrospective cases, respectively.

In the prospective case (1), our objective is to find target events with $M = M_{ET}$ that were followed by at least one event with $M \geq M_{ET}$ within the prescribed time and space window. Suppose we search the catalog for such a target event and find one. If the target event is found to be an early aftershock of a nearby event with $M > M_{ET}$, we do not want to include it in the counting. This is because of possible dominant influence of the earlier mainshock as well as the intense earthquake interactions in the early portion of the aftershock sequence, which obscure the possible role of the target event. For this early aftershock screening, we use a simple time–space screening method in which a time window of 30 days and a spherical distance window with radius R (in km) equal to twice the empirical rupture length (Wells and Coppersmith, 1994; i.e., $R = 2 \times 10^{-2.44+0.59M} + 20$) is used, in which M is the magnitude for a mainshock in the catalog. We only screen early large aftershocks in our selected catalog ($M \geq 7.0$ since 1920 and $7.0 > M \geq 6.0$ since 1965) instead of the full USGS-NEIC catalog, so it is different from full aftershock declustering. The number of retained target events followed by events with $M \geq M_{ET}$ that passed the screening is N_F.

More complex declustering methods (e.g., Zaliapin and Ben-Zion, 2016) have been shown to give similar counts for early large aftershock detection to fixed time and magnitude-dependent space search windows (e.g., Dascher-Cousineau *et al.*, 2020), so this simple procedure is sufficient for our purposes. For $M_{ET} = 6.0$, about 19% of all target events are found to be aftershocks, and the screened event percentage becomes very small by $M_{ET} = 7.0$ (Table S1, available in the supplemental material to this article). Late (post-30-day) large aftershocks, particularly for very large mainshocks, can still contribute to the
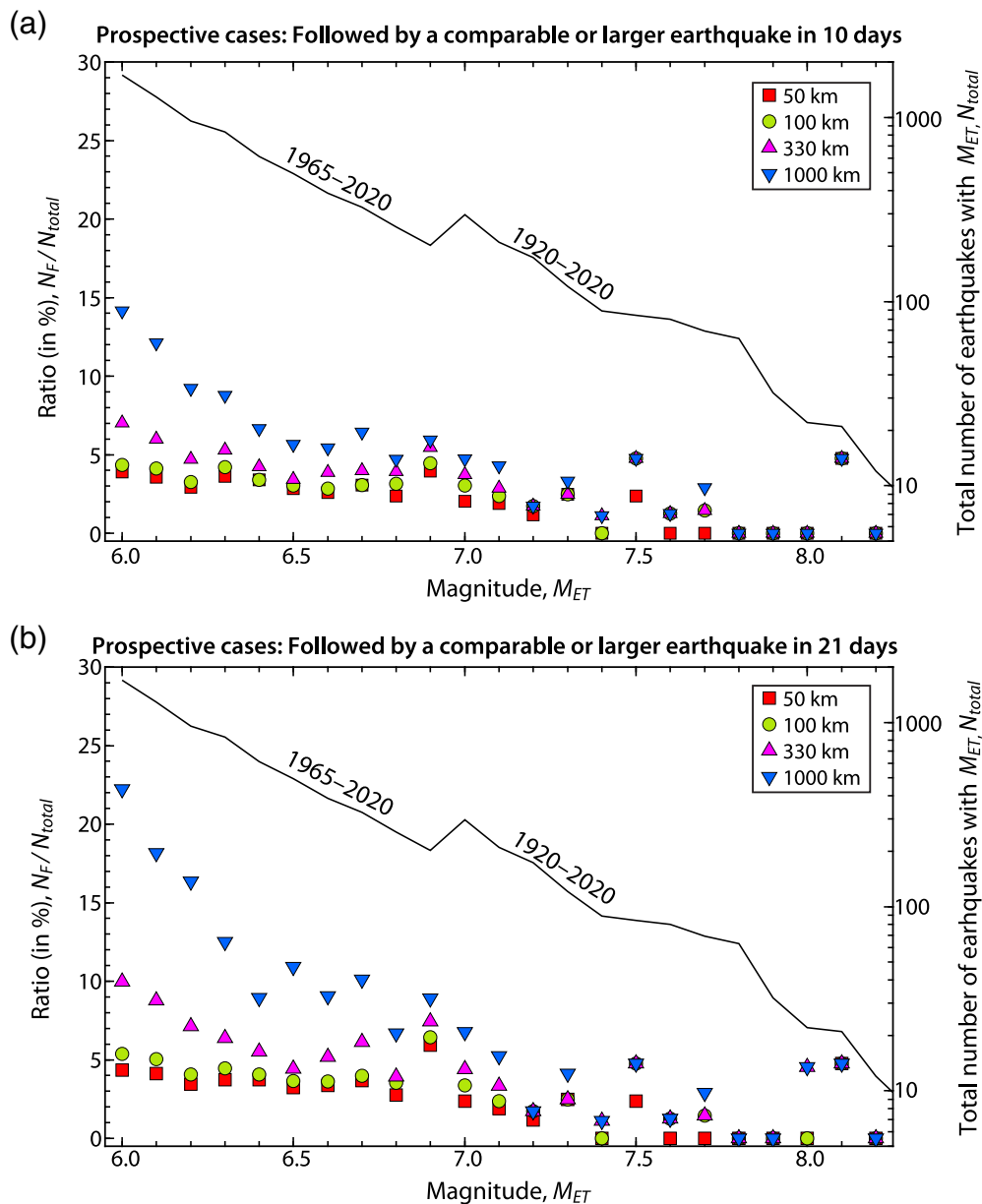
Figure 1. Historical prospective occurrence percentage for an earthquake (foreshock) followed by a larger event (mainshock) within different spherical radial distances (50–1000 km) over time ranges of (a) 10 days and (b) 21 days. For target events with magnitude $M_{ET} < 7.0$, the National Earthquake Information Center–U.S. Geological Survey (USGS-NEIC) catalog from 1 January 1965 to 2 November 2020 is used, whereas for $M_{ET} \geq 7$, the USGS-NEIC catalog from 1 January 1920 to 2 November 2020 is used. Black lines indicate the total number of earthquakes (right scale) with the given magnitude M_{ET} in the catalog time range. Colored symbols indicate the occurrence percentage of foreshock–mainshock pairs (left scale) found for different search distances. The color version of this figure is available only in the electronic edition.

The ratio N_F/N_{total} for target events with M_{ET} ranging from 6.0 to 8.2 is shown in Figure 1 for specified time windows ΔT of 10 days and 21 days and spherical windows centered on each target event with radii Δr varying from 50 to 1000 km. The ratios for small radii represent cases for which the target event would conventionally be identified as a foreshock (or doublet if $M \sim M_{ET}$), whereas for large radii the events could involve dynamic triggering or they could be physically independent. For M_{ET} ranging from 6.0 to 7.1, the ratios are about 4% with small radii of 50–100 km, although they increase for large radii due to more independent background and dynamic triggering cases. Major to great earthquakes were seldom followed by an even larger event in the last 100 yr (Table 1), with the most famous case being an M 8.1 event on 21 May 1960 (10:02:57 UTC) in Chile which was followed by the giant M 9.5 event on 22 May (19:11:20 UTC).

The total number of target events decreases with M_{ET}, as expected from the b-value being ~1.0 for the G-R relationship for the global catalog. There is a small jump in number of target events at $M_{ET} = 7.0$ due to expanding the duration of the catalog search back to 1920, but the slope of the expanded catalog distribution is about the same as for lower magnitudes. For events larger than ~7.5, there are relatively few events followed by comparable size or larger events within the specified distance and time windows. This leads to small sample sizes for large target magnitudes, and intrinsic fluctuations associated with the discrete magnitude intervals and the limited catalog duration.

counts, but such events tend to lie away from the rupture area of the earlier mainshock and are reasonably treated as target earthquakes in their own right as they are separated from the early intense aftershock activity. Screened event percentages for a 60-day aftershock window are shown in Table S1, with less than 0%–3% more target events for each magnitude being excluded.

TABLE 1

Historical Prospective Occurrence of an Event with Given Magnitude M_{ET} Being Followed by a Comparable or Larger Event in Specified Time and Space Windows

M_{ET}	N_{total}*	10 Days				21 Days			
		N_F (50)†	N_F (100)	N_F (330)	N_F (1000)	N_F (50)	N_F (100)	N_F (330)	N_F (1000)
6.0	1696	66 (10.4 ± 3.22)‡	74 (22.8 ± 4.74)	119 (79.9 ± 8.68)	240 (245.9 ± 19.62)	74 (21.5 ± 4.61)	91 (46.4 ± 6.69)	169 (158.8 ± 12.08)	377 (456.8 ± 44.68)
6.1	1288	46 (6.5 ± 2.50)	53 (14.4 ± 3.77)	77 (51.2 ± 6.99)	156 (151.5 ± 14.40)	53 (13.3 ± 3.53)	65 (29.5 ± 5.22)	113 (102.1 ± 9.55)	234 (287.1 ± 29.69)
6.2	955	28 (3.6 ± 1.89)	31 (8.0 ± 2.80)	45 (31.2 ± 5.41)	88 (93.5 ± 10.51)	33 (7.5 ± 2.71)	39 (16.5 ± 4.02)	68 (62.9 ± 7.48)	156 (180.8 ± 20.24)
6.3	832	30 (2.8 ± 1.66)	35 (5.9 ± 2.41)	44 (21.1 ± 4.49)	73 (63.8 ± 8.43)	31 (5.8 ± 2.39)	37 (12.1 ± 3.42)	53 (42.8 ± 6.27)	104 (125.1 ± 15.25)
6.4	**615**	**21 (1.5 ± 1.24)**	**21 (3.3 ± 1.81)**	**26 (11.9 ± 3.38)**	**41 (37.7 ± 6.32)**	**23 (3.2 ± 1.77)**	**25 (7.0 ± 2.59)**	**34 (24.5 ± 4.78)**	**55 (75.0 ± 10.51)**
6.5	495	14 (1.1 ± 1.05)	15 (2.3 ± 1.53)	17 (8.0 ± 2.82)	28 (24.3 ± 5.00)	16 (2.3 ± 1.51)	18 (4.9 ± 2.18)	22 (16.4 ± 3.96)	54 (48.5 ± 7.92)
6.6	387	10 (0.8 ± 0.90)	11 (1.7 ± 1.29)	15 (5.5 ± 2.29)	21 (15.8 ± 3.93)	13 (1.6 ± 1.27)	14 (3.5 ± 1.83)	20 (11.2 ± 3.23)	35 (31.8 ± 6.01)
6.7	326	10 (0.5 ± 0.72)	10 (1.1 ± 1.02)	13 (3.4 ± 1.84)	21 (10.6 ± 3.25)	12 (1.1 ± 1.04)	13 (2.3 ± 1.47)	20 (7.1 ± 2.62)	33 (21.7 ± 4.85)
6.8	254	6 (0.3 ± 0.58)	8 (0.7 ± 0.84)	10 (2.3 ± 1.49)	12 (7.5 ± 2.74)	7 (0.7 ± 0.83)	9 (1.5 ± 1.21)	10 (4.7 ± 2.14)	17 (15.4 ± 4.03)
6.9	202	8 (0.2 ± 0.48)	9 (0.4 ± 0.62)	11 (1.3 ± 1.13)	12 (3.9 ± 1.99)	12 (0.5 ± 0.69)	13 (0.8 ± 0.88)	15 (2.7 ± 1.62)	18 (8.1 ± 2.87)
7.0	296	6 (0.3 ± 0.51)	9 (0.5 ± 0.71)	11 (1.7 ± 1.29)	14 (4.6 ± 2.15)	7 (0.6 ± 0.73)	10 (1.1 ± 1.01)	13 (3.5 ± 1.86)	20 (9.6 ± 3.16)
7.1	**210**	**4 (0.1 ± 0.38)**	**5 (0.3 ± 0.53)**	**6 (0.9 ± 0.92)**	**9 (2.7 ± 1.65)**	**4 (0.3 ± 0.54)**	**5 (0.6 ± 0.76)**	**7 (1.8 ± 1.31)**	**11 (5.7 ± 2.38)**
7.2	173	2 (0.1 ± 0.27)	3 (0.2 ± 0.40)	3 (0.6 ± 0.75)	3 (1.8 ± 1.31)	2 (0.2 ± 0.39)	3 (0.3 ± 0.58)	3 (1.2 ± 1.08)	3 (3.6 ± 1.89)
7.3	**121**	**3 (0.0 ± 0.18)**	**3 (0.1 ± 0.28)**	**3 (0.2 ± 0.49)**	**4 (0.7 ± 0.85)**	**3 (0.1 ± 0.26)**	**3 (0.2 ± 0.41)**	**3 (0.5 ± 0.68)**	**5 (1.5 ± 1.24)**
7.4	**89**	**0 (0.0 ± 0.18)**	**0 (0.1 ± 0.29)**	**1 (0.2 ± 0.45)**	**1 (0.5 ± 0.72)**	**0 (0.1 ± 0.26)**	**0 (0.2 ± 0.42)**	**1 (0.4 ± 0.64)**	**1 (1.1 ± 1.04)**
7.5	**84**	**2 (0.0 ± 0.18)**	**4 (0.1 ± 0.27)**	**4 (0.1 ± 0.38)**	**4 (0.5 ± 0.68)**	**2 (0.1 ± 0.26)**	**4 (0.2 ± 0.40)**	**4 (0.3 ± 0.56)**	**4 (1.0 ± 0.99)**
7.6	80	0 (0.0 ± 0.13)	1 (0.1 ± 0.23)	1 (0.1 ± 0.38)	1 (0.4 ± 0.59)	0 (0.0 ± 0.20)	1 (0.1 ± 0.34)	1 (0.3 ± 0.54)	1 (0.8 ± 0.85)
7.7	69	0 (0.0 ± 0.15)	1 (0.1 ± 0.24)	1 (0.1 ± 0.31)	2 (0.2 ± 0.45)	0 (0.0 ± 0.21)	1 (0.1 ± 0.35)	1 (0.2 ± 0.45)	2 (0.4 ± 0.66)
7.8	63	0 (0.0 ± 0.12)	0 (0.0 ± 0.16)	0 (0.1 ± 0.26)	0 (0.2 ± 0.42)	0 (0.0 ± 0.17)	0 (0.1 ± 0.23)	0 (0.1 ± 0.37)	0 (0.4 ± 0.61)
7.9	32	0 (0.0 ± 0.00)	0 (0.0 ± 0.07)	0 (0.0 ± 0.20)	0 (0.1 ± 0.26)	0 (0.0 ± 0.00)	0 (0.0 ± 0.10)	0 (0.1 ± 0.29)	0 (0.1 ± 0.36)
8.0	22	0 (0.0 ± 0.00)	0 (0.0 ± 0.00)	0 (0.0 ± 0.07)	0 (0.0 ± 0.12)	0 (0.0 ± 0.00)	0 (0.0 ± 0.00)	0 (0.0 ± 0.11)	1 (0.0 ± 0.17)
8.1	**21**	**1 (0.0 ± 0.07)**	**1 (0.0 ± 0.10)**	**1 (0.0 ± 0.12)**	**1 (0.0 ± 0.15)**	**1 (0.0 ± 0.11)**	**1 (0.0 ± 0.14)**	**1 (0.0 ± 0.17)**	**1 (0.1 ± 0.22)**
8.2	12	0 (0.0 ± 0.00)	0 (0.0 ± 0.00)	0 (0.0 ± 0.08)	0 (0.0 ± 0.13)	0 (0.0 ± 0.00)	0 (0.0 ± 0.00)	0 (0.0 ± 0.11)	0 (0.0 ± 0.18)

Specific cases discussed in the Discussion section are given in bold.

*Total number of target events: For target events with magnitude $M_{ET} < 7.0$, the National Earthquake Information Center at U.S. Geological Survey (USGS-NEIC) catalog from 1 January 1965 to 2 November 2020 is used, whereas for $M_{ET} \geq 7$, the USGS-NEIC catalog from 1 January 1920 to 2 November 2020 is used.

†Number of target events with M_{ET} within the given radii ranging from 50 to 1000 km.

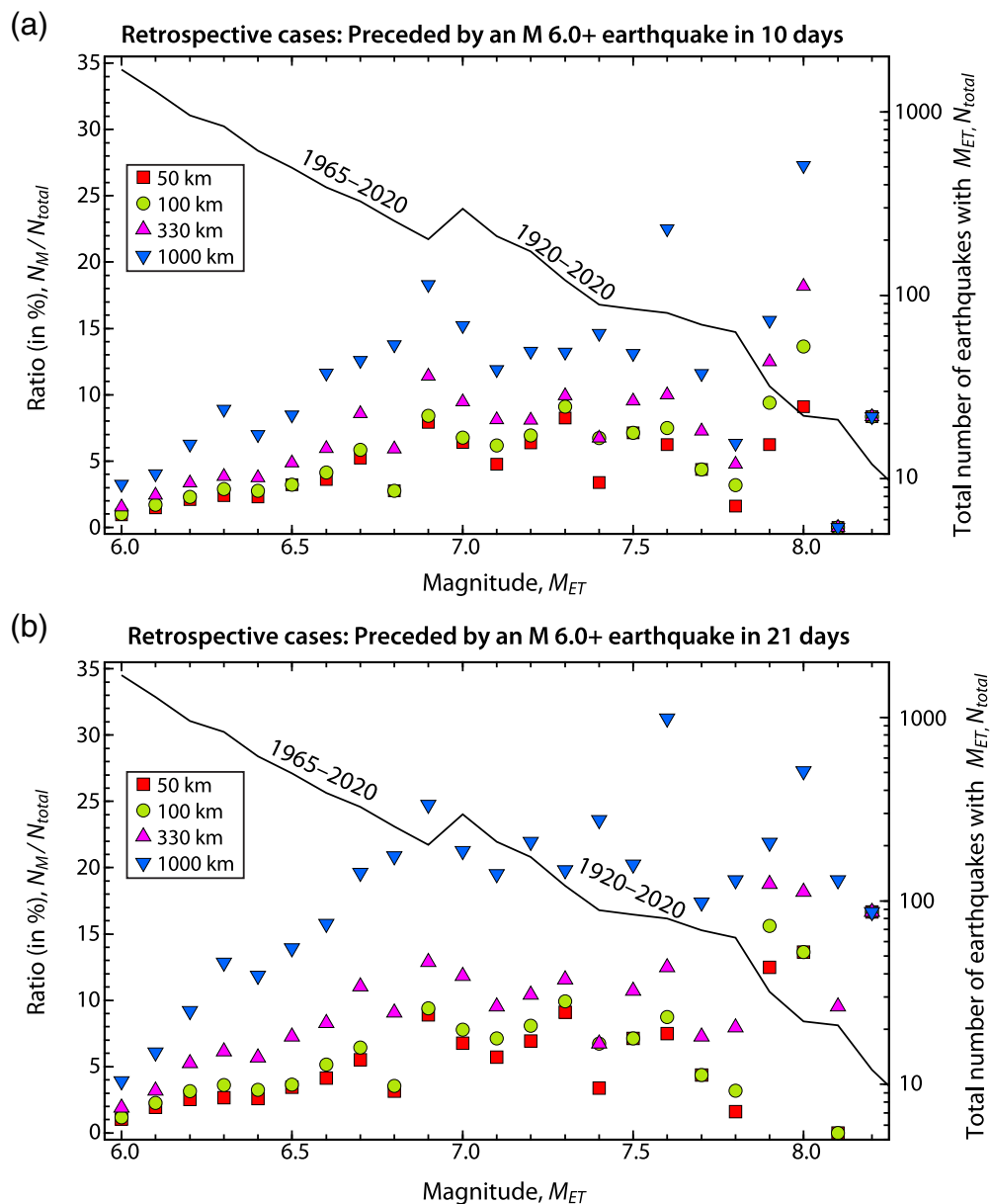‡The average value and one standard deviation of corresponding occurrences in 9999 time-randomized catalog searches.

Figure 2. Historical retrospective occurrence percentage for an earthquake (mainshock) with the given magnitude preceded by an M 6.0+ event (foreshock) within different radial distances (50–1000 km) over time ranges of (a) 10 days and (b) 21 days. Colored symbols indicate the occurrence percentage for foreshock–mainshock pairs (left scale) found for different search distances. Other symbols are the same as Figure 1. The color version of this figure is available only in the electronic edition.

distance may have dynamically triggered the target event, or they could be physically independent.

Discussion

The distributions in Figures 1 and 2 can be quickly calculated for any spatial window, time window, and magnitude for a catalog with $M \geq 6.0$, as only a few thousand total events are included. This facilitates responding to any specific inquiry. The specific time intervals of 10 and 21 days are just illustrative. The truncated catalog and search algorithm are presented in the supplemental material. The results are for a global catalog and do not provide any region-specific information, although it can be easily implemented in the programming package provided in the supplemental material.

For both prospective (Fig. 1) and retrospective cases (Fig. 2), the curves for larger search radii move upward to higher counts. This does not signify greater likelihood of causal interactions between events and is largely because larger sampling of seismogenic areas increases the event counts in the space–time window. To account for this intrinsic nature of Earth's seismicity, we perform the same processing on catalogs with 9999 realizations of randomized

In the retrospective case (2), let N_M be the number of events with $M = M_{ET}$ that were preceded by at least one event with $6.0 \leq M \leq M_{ET}$, after ruling out either event in the pair as being an early aftershock or a selected event in the prospective case defined previously. The ratio N_M/N_{total} for the target event with M_{ET} ranging from 6.0 to 8.3 is shown in Figure 2 for specified time windows ΔT of 10 and 21 days and spherical windows centered on each target event with radii Δr varying from 50 to 1000 km. In this case, the ratios increase with M_{ET}, as well as with the spatial range of the search. Events at larger

timing of actual events for an interval ± 2.5 yr around each target event. The event magnitude distribution is preserved, as are locations, so this process eliminates any actual foreshock or aftershock relationships, but preserves the basic spatial and magnitude distribution of global seismicity. Corresponding curves are shown in Figures S1 and S2 for the prospective and retrospective cases, respectively. These curves demonstrate the expected behavior of the measures with increasing search radius and target event size intrinsic to global seismicity distributions devoid of actual foreshock and aftershock clustering.
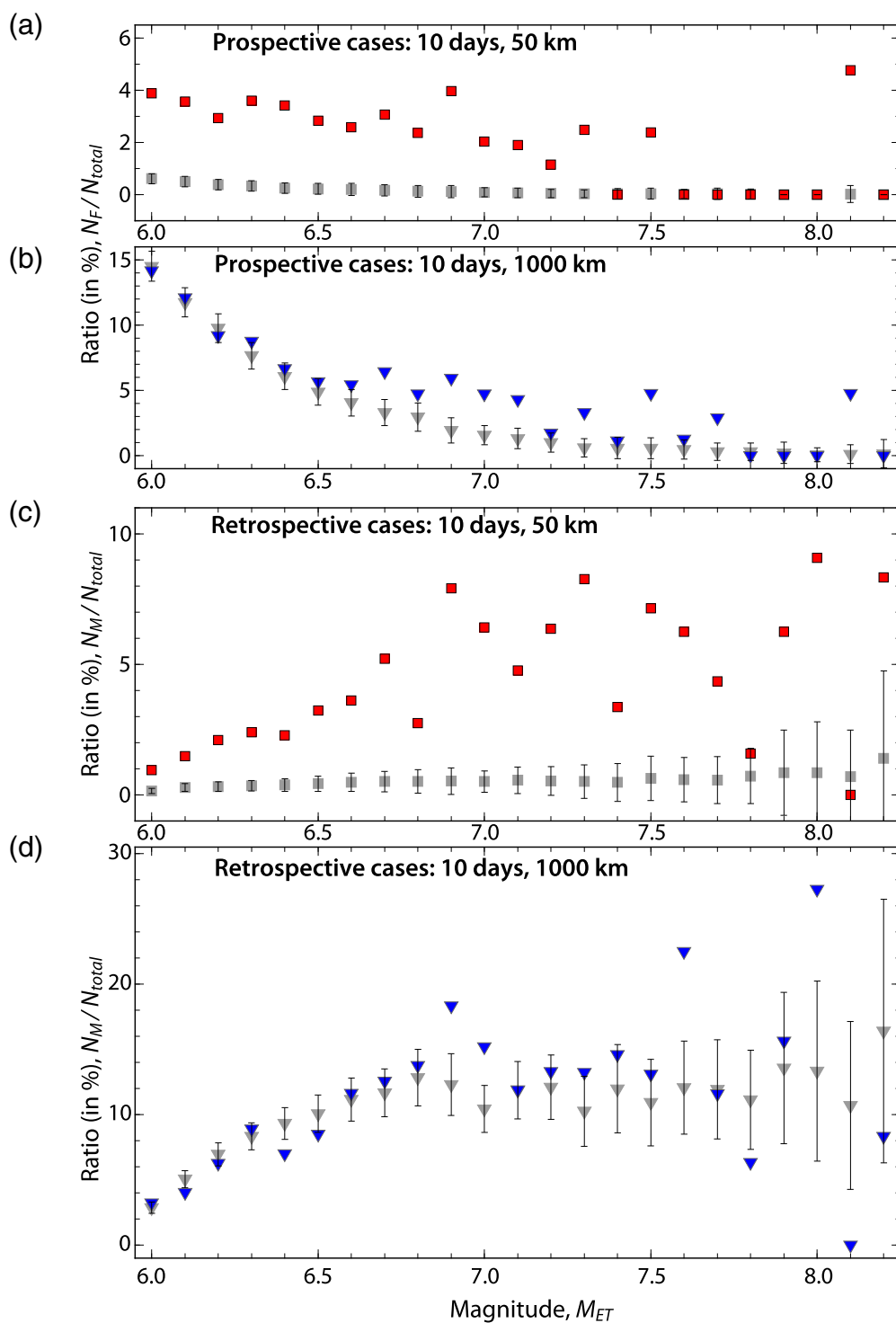
Figure 3. Comparison of (a,b) prospective and (c,d) retrospective occurrence percentages with values from temporally randomized catalogs within radial distances of (a,c) 50 km and (b,d) 1000 km. Colored symbols indicate percentage for foreshock–mainshock pairs within 10 days from the USGS-NEIC catalog, whereas gray ones indicate corresponding average values from 9999 temporally randomized catalogs. The color version of this figure is available only in the electronic edition.

cases. When actual catalog values give higher percentages of observed counts than the randomized distribution, one can infer a corresponding gain in likelihood of causal interaction relative to random distribution for the global seismicity. Comparisons for the 100 and 330 km cases are provided in Figure S3.

So, how could these distributions be used to respond to challenging inquiries about possible earthquake interactions? If asked a prospective question such as how likely it is that a magnitude 6.4 earthquake (e.g., the 4 July 2019 Ridgecrest foreshock) which has just occurred is a foreshock of a forthcoming event of equal size or larger within 100 km in the next 10 days, one can refer to Table 1 and the prospective curve in Figure 1a to state that "among 615 global occurrences of earthquakes of this size from 1965 to 2020, 21 events (about 4%) that are not early aftershocks have been followed by a comparable size or larger event within 10 days and 100 km" (Table 1; given in italics). Referring to Figure S1 and Table 1, the caveat could be given that "a random catalog would give two such cases (about 0.5%)." If a fully developed OEF result is available in a well-calibrated region, a more precise probabilistic answer for prospective events of different size can be provided, but the simple statement earlier provides a reasonably understandable context of low, but nonzero potential for a larger event to happen based on historical global observations, qualified by nature of Earth's overall seismicity distribution. If the concern was with regard to possible occurrence of a large event far from the first event (perhaps along southern Cascadia

Figure 3 compares actual catalog results with the randomized ensemble results for a search radius of 10 days for 50 and 1000 km search ranges for both prospective and retrospective

TABLE 2
Historical Retrospective Occurrence of an Event with Given Magnitude M_{ET} Being Preceded by an M 6.0+ Event in Specified Time and Space Windows

M_{ET}	N_{total}*	10 Days				21 Days			
		N_M (50)†	N_M (100)	N_M (330)	N_M (1000)	N_M (50)	N_M (100)	N_M (330)	N_M (1000)
6.0	1696	16 (2.5 ± 1.59)‡	17 (5.2 ± 2.28)	26 (16.8 ± 4.07)	55 (48.3 ± 7.30)	18 (5.1 ± 2.24)	20 (10.5 ± 3.19)	32 (31.9 ± 5.54)	66 (79.4 ± 11.11)
6.1	1288	19 (3.7 ± 1.87)	22 (7.3 ± 2.65)	31 (23.8 ± 4.76)	52 (65.1 ± 8.37)	25 (7.4 ± 2.63)	29 (14.6 ± 3.72)	41 (45.0 ± 6.50)	78 (108.6 ± 13.54)
6.2	955	20 (3.0 ± 1.72)	22 (6.6 ± 2.56)	32 (23.5 ± 4.69)	60 (66.4 ± 8.53)	24 (6.1 ± 2.45)	30 (13.2 ± 3.58)	50 (44.6 ± 6.44)	88 (112.7 ± 13.91)
6.3	832	20 (2.9 ± 1.70)	24 (6.6 ± 2.53)	32 (24.5 ± 4.76)	74 (69.4 ± 8.59)	22 (6.0 ± 2.44)	30 (13.3 ± 3.54)	51 (46.5 ± 6.37)	107 (119.4 ± 14.26)
6.4	615	14 (2.3 ± 1.50)	17 (5.1 ± 2.20)	23 (19.4 ± 4.20)	43 (57.7 ± 7.62)	16 (4.8 ± 2.14)	20 (10.3 ± 3.12)	35 (37.9 ± 5.73)	73 (101.6 ± 12.48)
6.5	495	16 (2.1 ± 1.44)	16 (4.7 ± 2.13)	24 (17.0 ± 3.97)	42 (50.0 ± 7.15)	17 (4.4 ± 2.08)	18 (9.6 ± 3.00)	36 (33.0 ± 5.34)	69 (88.9 ± 11.38)
6.6	387	14 (1.9 ± 1.35)	16 (4.1 ± 2.00)	23 (15.0 ± 3.73)	45 (43.3 ± 6.42)	16 (3.8 ± 1.92)	20 (8.4 ± 2.83)	32 (29.3 ± 5.03)	61 (77.1 ± 10.08)
6.7	326	17 (1.6 ± 1.27)	19 (3.7 ± 1.90)	28 (12.5 ± 3.39)	41 (37.8 ± 5.95)	18 (3.4 ± 1.83)	21 (7.6 ± 2.68)	36 (24.6 ± 4.56)	64 (67.9 ± 9.18)
6.8	254	7 (1.3 ± 1.15)	7 (3.0 ± 1.70)	15 (10.4 ± 3.14)	35 (32.7 ± 5.50)	8 (2.7 ± 1.61)	9 (6.1 ± 2.37)	23 (20.6 ± 4.19)	53 (58.9 ± 8.21)
6.9	202	16 (1.1 ± 1.03)	17 (2.1 ± 1.44)	23 (8.0 ± 2.75)	37 (25.0 ± 4.80)	18 (2.2 ± 1.48)	19 (4.3 ± 2.04)	26 (15.8 ± 3.72)	50 (45.7 ± 6.96)
7.0	296	19 (1.5 ± 1.20)	20 (3.3 ± 1.79)	28 (10.9 ± 3.15)	45 (30.8 ± 5.29)	20 (3.1 ± 1.70)	23 (6.8 ± 2.51)	35 (21.6 ± 4.24)	63 (56.4 ± 7.95)
7.1	**210**	**10 (1.2 ± 1.07)**	**13 (2.7 ± 1.60)**	**17 (8.5 ± 2.74)**	**25 (25.0 ± 4.63)**	**12 (2.4 ± 1.53)**	**15 (5.5 ± 2.28)**	**20 (16.8 ± 3.71)**	**41 (45.6 ± 6.80)**
7.2	173	11 (0.9 ± 0.96)	12 (2.1 ± 1.43)	14 (7.4 ± 2.60)	23 (21.2 ± 4.31)	12 (2.0 ± 1.39)	14 (4.4 ± 2.03)	18 (14.8 ± 3.52)	38 (39.1 ± 6.16)
7.3	121	10 (0.6 ± 0.78)	11 (1.4 ± 1.15)	12 (4.4 ± 1.96)	16 (12.4 ± 3.23)	11 (1.3 ± 1.11)	12 (2.8 ± 1.60)	14 (8.5 ± 2.58)	24 (23.2 ± 4.46)
7.4	89	3 (0.4 ± 0.65)	6 (0.9 ± 0.98)	6 (3.5 ± 1.80)	13 (10.6 ± 2.98)	3 (0.9 ± 0.94)	6 (2.0 ± 1.38)	6 (7.0 ± 2.45)	21 (19.7 ± 4.04)
7.5	84	6 (0.5 ± 0.72)	6 (1.1 ± 0.99)	8 (2.8 ± 1.59)	11 (9.2 ± 2.80)	6 (1.1 ± 1.02)	6 (2.2 ± 1.40)	9 (5.7 ± 2.19)	17 (17.3 ± 3.73)
7.6	80	5 (0.5 ± 0.68)	6 (0.9 ± 0.94)	8 (2.8 ± 1.63)	18 (9.6 ± 2.85)	6 (1.0 ± 0.95)	7 (1.9 ± 1.33)	10 (5.8 ± 2.22)	25 (18.1 ± 3.79)
7.7	69	3 (0.4 ± 0.62)	3 (0.9 ± 0.93)	5 (2.8 ± 1.56)	8 (8.3 ± 2.63)	3 (0.8 ± 0.89)	3 (1.9 ± 1.31)	5 (5.5 ± 2.08)	12 (15.4 ± 3.48)
7.8	63	1 (0.5 ± 0.67)	2 (1.0 ± 0.99)	3 (2.8 ± 1.59)	4 (7.0 ± 2.40)	1 (1.0 ± 0.96)	2 (2.1 ± 1.39)	5 (5.6 ± 2.16)	12 (13.2 ± 3.20)
7.9	32	2 (0.3 ± 0.52)	3 (0.6 ± 0.77)	4 (1.9 ± 1.29)	5 (4.3 ± 1.86)	4 (0.6 ± 0.73)	5 (1.3 ± 1.07)	6 (3.6 ± 1.67)	7 (7.9 ± 2.32)
8.0	22	2 (0.2 ± 0.43)	3 (0.5 ± 0.66)	4 (1.3 ± 1.07)	6 (2.9 ± 1.52)	3 (0.4 ± 0.62)	3 (0.9 ± 0.91)	4 (2.5 ± 1.39)	6 (5.4 ± 1.88)
8.1	21	0 (0.1 ± 0.38)	0 (0.4 ± 0.60)	0 (1.1 ± 0.99)	0 (2.3 ± 1.36)	0 (0.3 ± 0.54)	0 (0.8 ± 0.84)	2 (2.2 ± 1.32)	4 (4.3 ± 1.75)

Specific cases discussed in the Discussion section are given in bold.

*Total number of target events: For target events with magnitude $M_{ET} < 7.0$, the USGS-NEIC catalog from 1 January 1965 to 2 November 2020 is used, whereas for $M_{ET} \geq 7$, the USGS-NEIC catalog from 1 January 1920 to 2 November 2020 is used.

†Number of target events with M_{ET} within the given radii ranging from 50 to 1000 km.

‡The average value and one standard deviation of corresponding occurrences in 9999 time-randomized catalog searches.

(Continued next page.)

TABLE 2 (continued)
Historical Retrospective Occurrence of an Event with Given Magnitude M_{ET} Being Preceded by an M 6.0+ Event in Specified Time and Space Windows

M_{ET}	N_{total}*	10 Days				21 Days			
		$N_M(50)$†	$N_M(100)$	$N_M(330)$	$N_M(1000)$	$N_M(50)$	$N_M(100)$	$N_M(330)$	$N_M(1000)$
8.2	12	1 (0.2 ± 0.40)	1 (0.3 ± 0.55)	1 (0.7 ± 0.79)	1 (2.0 ± 1.21)	2 (0.3 ± 0.56)	2 (0.7 ± 0.74)	2 (1.4 ± 1.04)	2 (3.5 ± 1.45)
8.3	8	1 (0.1 ± 0.37)	1 (0.3 ± 0.53)	1 (0.6 ± 0.73)	2 (1.2 ± 0.97)	1 (0.3 ± 0.52)	1 (0.6 ± 0.74)	1 (1.2 ± 0.95)	2 (2.2 ± 1.19)
8.4	4	0 (0.0 ± 0.10)	1 (0.1 ± 0.22)	1 (0.2 ± 0.46)	2 (0.5 ± 0.65)	0 (0.0 ± 0.14)	1 (0.1 ± 0.32)	1 (0.5 ± 0.64)	2 (0.9 ± 0.83)
8.5	**3**	**1 (0.0 ± 0.16)**	**1 (0.1 ± 0.32)**	**2 (0.2 ± 0.42)**	**2 (0.4 ± 0.56)**	**1 (0.1 ± 0.23)**	**1 (0.2 ± 0.43)**	**2 (0.4 ± 0.54)**	**2 (0.7 ± 0.66)**
8.6	5	0 (0.1 ± 0.27)	0 (0.1 ± 0.37)	0 (0.5 ± 0.65)	0 (1.0 ± 0.86)	0 (0.2 ± 0.39)	0 (0.3 ± 0.51)	0 (1.0 ± 0.82)	0 (1.8 ± 0.99)
8.7	1	0 (0.0 ± 0.06)	0 (0.0 ± 0.13)	0 (0.1 ± 0.26)	0 (0.2 ± 0.37)	0 (0.0 ± 0.09)	0 (0.0 ± 0.18)	0 (0.1 ± 0.35)	0 (0.3 ± 0.46)
8.8	1	0 (0.0 ± 0.16)	0 (0.1 ± 0.23)	0 (0.2 ± 0.36)	0 (0.2 ± 0.39)	0 (0.1 ± 0.23)	0 (0.1 ± 0.33)	0 (0.3 ± 0.46)	0 (0.4 ± 0.48)
9.0	1	0 (0.1 ± 0.25)	0 (0.1 ± 0.35)	0 (0.3 ± 0.46)	0 (0.4 ± 0.50)	0 (0.1 ± 0.35)	0 (0.3 ± 0.45)	0 (0.5 ± 0.50)	0 (0.7 ± 0.46)
9.1	**2**	**1 (0.0 ± 0.19)**	**1 (0.1 ± 0.35)**	**1 (0.5 ± 0.58)**	**1 (0.7 ± 0.67)**	**1 (0.1 ± 0.27)**	**1 (0.3 ± 0.48)**	**1 (0.8 ± 0.65)**	**1 (1.2 ± 0.69)**
9.2	1	0 (0.0 ± 0.00)	0 (0.0 ± 0.10)	0 (0.1 ± 0.28)	0 (0.2 ± 0.40)	0 (0.0 ± 0.00)	0 (0.0 ± 0.15)	0 (0.2 ± 0.38)	0 (0.4 ± 0.48)
9.5	**1**	**1 (0.0 ± 0.18)**	**1 (0.1 ± 0.27)**	**1 (0.1 ± 0.31)**	**1 (0.2 ± 0.39)**	**1 (0.1 ± 0.27)**	**1 (0.2 ± 0.37)**	**1 (0.2 ± 0.41)**	**1 (0.4 ± 0.48)**

Specific cases discussed in the Discussion section are given in bold.

*Total number of target events: For target events with magnitude $M_{ET} < 7.0$, the USGS-NEIC catalog from 1 January 1965 to 2 November 2020 is used, whereas for $M_{ET} \geq 7$, the USGS-NEIC catalog from 1 January 1920 to 2 November 2020 is used.

†Number of target events with M_{ET} within the given radii ranging from 50 to 1000 km.

‡The average value and one standard deviation of corresponding occurrences in 9999 time-randomized catalog searches.

for an M 6.4 event in southern California), the catalog (Table 1) shows that "41 (about 7%) of such size events that are not early aftershocks have been followed by a comparable or larger event within 10 days and 1000 km," "but a random catalog would predict about 38 such events on average" (Table 1). Whether the range of values in the random catalog is valuable to convey or not depends on the goal of the communication, and usually is most important for long-range interactions. Typically, OEF statistical results are not well calibrated for such long-range interactions, so Figures 1 and 2 provide a catalog-based distillation of historical earthquake occurrence that conveys the fact that remote triggering interactions do occur but still have low frequency of occurrence, whereas Figure 3 accounts for the effects of Earth's seismicity distribution.

Asked a retrospective question about causal connection between a recent large event (say, of $M_{ET} = 7.1$) and prior events within the last three weeks at various distances (nearby or far away), Figures 2 and 3 provide a response that "the catalog shows that among 210 events of this size from 1920 to 2020, 12 events (about 6%) that are not early aftershocks have been preceded by an event larger than 6.0 within 50 km within 21 days (a random catalog would give two events [about 1%] on average), and 41 events (around 20%) that are not early aftershocks have been preceded by an event larger than 6.0 within 1000 km (a random catalog would give 46 events [about 22%] on average, Fig. S2)" (Table 2). Of course, the large spatial scale samples a vast area, so the event count is larger due to inclusion of more, probably unrelated events, and that is accounted for by reference to the random catalog. However, the reality is that each of the events could have involved some dynamic interaction with the recent event. As we generally do not have the ability to quantitatively define which events dynamically interact, conveying the history of occurrences is a reasonable approach that can be understood without a formal statistical parameterization of earthquake sequences.

Finally, we provide an additional prospective case scenario based on the 13 February 2021 M_w 7.1 Fukushima earthquake (we use the USGS-NEIC estimate). Given a media or public inquiry about the possibility of a subsequent larger earthquake happening within 10 days and 100 km, our suggested response would be as following: "Among 210 global occurrences of earthquakes of this size (M_w 7.1) from 1920 to 2020, five events (about 2.4%) that are not early aftershocks of larger events have been followed by a comparable size or larger event within 10 days and 100 km" (this information is directly taken from Table 1). More detailed information can also be provided from the output of the code provided in the supplemental material, if asked for specific cases:

1. an M_w 7.1 in 11 April 2014 in Papua New Guinea followed by an M_w 7.5 at ~26 km and 8 days;
2. an M_w 7.1 in 17 May 1992 in Mindanao followed by an M_w 7.3 at ~14 km and ~30 min;
3. an M_w 7.1 in 16 April 1963 in Indonesia followed by an M_w 7.1 at ~9 km and ~25 min;
4. an M 7.1 in 24 April 1957 in Greece followed by an M 7.3 at ~15 km and ~7 hr; and
5. an M 7.1 in 14 April 1928 in Bulgaria followed by an M 7.1 at 50 km and 4.4 days.

From Table 1 and Figure 1, the occurrence percentage is about 2%–3% for the time windows of 2–3 weeks and distance ranges of 50–300 km, and it increases to be about 5% if we consider a larger distance range up to 1000 km. From a large ensemble of randomized catalogs, on average about 0.3 events of the total 210 events (about 0.1%) with M_w 7.1 are followed by a larger earthquake within 10 days and 100 km, and 5.7 events (about 2.7%) for 21 days and 1000 km. Again, the specific question from the media and public determines how much of this information would be provided. Our procedure provides simple access to the catalog basis for reliably answering such a question with ready flexibility as to the specific catalog, magnitude, time, and spatial extent. It is very important to give the public a general sense for the total sample size and background seismicity level underlying any response to their inquiry for them to develop a general understanding of the numbers and occurrence percentages provided.

Of course, providing this information in response to typical initial inquiries may form only the starting basis of a longer discussion with the media, and they may well ask many follow-up questions, but the intent is for them to have a take-home message based on the typically low occurrence percentages of seismological experience. Clarity in initial response will prevent the follow-up questions from focusing on technical complexities and confusion over probabilistic vernacular, and this will help the overall communication. For the 2021 Fukushima event, important additional information in a follow-up discussion may be that the event can be considered to be a late (~10 yr) aftershock of the 2011 M_w 9.1 Tohoku earthquake, based on sustained elevated seismicity rates relative to the interval before that event. The event was only the second event since 11 March 2011 to produce greater than Japan Meteorological Agency intensity VI shaking levels in the epicentral area of the 2011 M_w 9.1 event. The strong ground shaking from the 2021 Fukushima is probably due to the combination of energetic process from the intraplate rupture and less attenuation of seismic waves along the path upward to the surface, similar to the 7 April 2011 M_w 7.1 Tohoku intraplate earthquake (e.g., Ye et al., 2013). Even if viewed as a late aftershock, there is no reason that this event could not trigger another event, so our procedure is valid for providing a response to the public.

Another caveat in this analysis is raised from the sparseness of large event pairs in our 100 yr catalog and uncertainty in magnitude determination over time. For example, based on the recent 4 March 2021 M_w 7.4 and 8.1 Kermadec Islands

events, with separation of 47 min in time and 105 km in distance between two large earthquakes, we consider prospective and retrospective questions for target magnitudes of M_w 7.4 and 8.1, respectively, within 10 days at distance range of 100 km. For the total of 89 M_w 7.4 earthquakes in the USGS-NEIC catalog from 1920 to 2 November 2020 used in this study, none (that are not early aftershocks) were followed by an equal or larger event. For the total of 21 M_w 8.1 events, none were preceded by an M 6.0+ foreshock in 10 days and 100 km. Against to deal with the small sample size for these large magnitudes, one could smooth the frequency over adjacent magnitude bins. For example, three of 121 M_w 7.3 events and four of 84 M_w 7.5 events that are not early aftershocks were followed by an equal or larger event in 10 days and 100 km, so for a reference magnitude of M_w 7.4, one might say that seven events out 294 events (about 2.4%) with M_w 7.3–7.5 that are not early aftershocks are followed by an equal or larger event. Retrospectively, we can sum up with the three of 22 M_w 8.0 events and one of 12 M_w 8.2 events preceded by an M 6.0+ foreshock, to get state that four events out of 55 M_w 8.0–8.3 events had at least one M 6.0+ foreshock. Of course, numbers of target events and foreshock–mainshock pairs will be updated gradually with time, so this caveat will diminish.

Future efforts could involve developing a convenient app or webpage for making specific responses to the public. Of course, given information about the source dynamics, more quantitative approaches such as observing or computing ground shaking at the target site and the history of seismicity rate increases at corresponding shaking levels may be pursued (e.g., van der Elst and Brodsky, 2010), but this is not typically readily available. It would also be valuable to engage in the future with social scientists in the most effective dissemination of seismological information about large earthquake interactions from all technical procedures in response to public inquiries.

Data and Resources

Declaration of Competing Interests

The authors acknowledge there are no conflicts of interest recorded.

Acknowledgments

References

Bayona Viveros, J. A., S. von Specht, A. Strader, S. Hainzl, F. Cotton, and D. Schorlemmer (2019). A regionalized seismicity model for subduction zones based on geodetic strain rates, geomechanical parameters, and earthquake-catalog data, Bull. Seismol. Soc. Am. 109, 2036–2049, doi: 10.1785/0120190034.

Bird, P., and C. Kreemer (2015). Revised tectonic forecast of global shallow seismicity based on version 2.1 of the Global Strain Rate Map, Bull. Seismol. Soc. Am. 105, 152–166.

Dascher-Cousineau, K., E. E. Brodsky, T. Lay, and T. H. W. Goebel (2020). What controls variations in aftershock productivity? J. Geophys. Res. 125, e2019JB018111, doi: 10.1029/2019JB018111.

Field, E. H., T. H. Jordan, L. M. Jones, A. J. Michael, M. L. Blanpied, and Other Workshop Participants (2016). The potential uses of operational earthquake forecasting, Seismol. Res. Lett. 87, 313–322, doi: 10.1785/0220150174.

Field, E. H., K. R. Milner, J. L. Hardebeck, M. T. Page, N. van der Elst, T. H. Jordan, A. J. Michael, B. E. Shaw, and M. J. Werner (2017). A spatiotemporal clustering model for the third Uniform California Earthquake Rupture Forecast (UCERF3-ETAS): Toward an operational earthquake forecast, Bull. Seismol. Soc. Am. 107, 1049–1081, doi: 10.1785/0120160173.

Fukushima, Y., and T. Nishikawa (2020). New earthquake warning framework in the Nankai Trough subduction zone in Japan and scientific rationale that the society need to know for effective countermeasures, American Geophysical Union, Abstract NH018-0007.

Gutenberg, B., and C. F. Richter (1944). Frequency of earthquakes in California, Bull. Seismol. Soc. Am. 4, 185–188.

Jordan, T. H., and L. M. Jones (2010). Operational earthquake forecasting: Some thoughts on why and how, Seismol. Res. Lett. 81, no. 4, 571–574, doi: 10.1785/gssrl.81.4.571.

Jordan, T. H., Y.-T. Chen, P. Gasparini, R. Madariaga, I. Main, W. Marzocchi, G. Papadopoulos, G. Sobolev, K. Yamaoka, and J. Zschau (2011). Operational earthquake forecasting: State of knowledge and guidelines for implementation. International Commission on Earthquake Forecasting for Civil Protection, Ann. Geophys. 54, no, 4, 315–391, doi: 10.4401/ag-5350.

Jordan, T. H., W. Marzocchi, A. J. Michael, and M. C. Gerstenberger (2014). Operational earthquake forecasting can enhance earthquake preparedness, Seismol. Res. Lett. 85, 955–959, doi: 10.1785/0220140143.

Kagan, Y. Y. (2003). Accuracy of modern global earthquake catalogs, Phys. Earth Planet. In. 135, 173–209.

Kagan, Y. Y. (2017). Worldwide earthquake forecasts, Stoch. Environ. Res. Risk Assess. 31, 1273–1290, doi: 10.1007/s00477-016-1268-9.

Kamaya, N., K. Takeda, and T. Hashimoto (2017). New Japanese guidelines for the information of the prospect of seismic activity

after large earthquakes and their applications, *J. Disast. Res.* **12,** 1109–1116.

Michael, A. J. (2014). How complete is the ISC-GEM global earthquake catalog? *Bull. Seismol. Soc. Am.* **104,** 1829–1837, doi: 10.1785/0120130227.

Ogata, Y. (1988). Statistical models for earthquake occurrences and residual analysis for point processes, *J. Am. Stat. Assoc.* **83,** 9–27.

Parsons, T., M. Segou, and W. Marzocchi (2014). The global aftershock zone, *Tectonophysics* **618,** 1–34, doi: 10.1016/j.tecto.2014.01.038.

Reasenberg, P. A., and L. M. Jones (1989). Earthquake hazard after a mainshock in California, *Science* **243,** 1173–1176.

Utsu, T., Y. Ogata, and R. S. Matsu'ura (1995). The centenary of the Omori formula for a decay law of aftershock activity, *J. Phys. Earth* **43,** 1–33.

van der Elst, N. J., and E. E. Brodsky (2010). Connecting near-field and far-field earthquake triggering to dynamic strain, *J. Geophys. Res.* **115,** no. B07311, doi: 10.1029/2009JB006681.

van der Elst, N. J., and M. T. Page (2018). Nonparametric aftershock forecasts based on similar sequences in the past, *Seismol. Res. Lett.* **89,** 145–152, doi: 10.1785/0220170155.

Velasco, A. A., S. Hernandez, T. Parsons, and K. Pankow (2008). Global ubiquity of dynamic earthquake triggering, *Nature Geosci.* **1,** 375–379, doi: 10.1038/ngeo204.

Wells, D. L., and K. J. Coppersmith (1994). New empirical relationships among magnitude, rupture length, rupture width, rupture area, and surface displacement, *Bull. Seismol. Soc. Am.* **84,** no. 4, 974–1002.

Wessel, P., W. H. Smith, R. Scharroo, J. Luis, and F. Wobbe (2013). Generic mapping tools: Improved version released, *Eos Trans. AGU* **94,** no. 45, 409–410.

Ye, L., T. Lay, and H. Kanamori (2013). Ground shaking and seismic source spectra for large earthquakes around the megathrust fault offshore of northeastern Honshu, Japan, *Bull. Seismol. Soc. Am.* **103,** no. 2B, 1221–1241.

Zaliapin, I., and Y. Ben-Zion (2016). A global classification and characterization of earthquake clusters, *Geophys. J. Int.* **207,** 608–634.